remote sensing

MDPI

Article

Tropical Species Classification with Structural Traits Using Handheld Laser Scanning Data

Meilian Wang [1], Man Sing Wong [1,2,*] and Sawaid Abbas [1,3]

[1] Department of Land Surveying and Geo-Informatics, The Hong Kong Polytechnic University, Hong Kong, China; meilianp.wang@connect.polyu.hk (M.W.); sawaid.abbas@connect.polyu.hk (S.A.)
[2] Research Institute of Land and Space, The Hong Kong Polytechnic University, Hong Kong, China
[3] Remote Sensing, GIS and Climatic Research Lab (RSGCRL), National Center of GIS and Space Applications, University of the Punjab, Lahore 54590, Pakistan
* Correspondence: ls.charles@polyu.edu.hk; Tel.: +852-3400-8959

Abstract: Information about tree species plays a pivotal role in sustainable forest management. Light detection and ranging (LiDAR) technology has demonstrated its potential to obtain species information using the structural features of trees. Several studies have explored the structural properties of boreal or temperate trees from terrestrial laser scanning (TLS) data and applied them to species classification, but the study of structural properties of tropical trees for species classification is rare. Compared to conventional static TLS, handheld laser scanning (HLS) is able to effectively capture point clouds of an individual tree with flexible movability. Therefore, in this study, we characterized the structural features of tropical species from HLS data as 23 LiDAR structural parameters, involving 6 branch, 11 crown and 6 entire tree parameters, and used these parameters to classify the species via 5 machine-learning (ML) models, respectively. The performance of each parameter was further evaluated and compared. Classification results showed that the employed parameters can achieve a classification accuracy of 84.09% using the support vector machine with a polynomial kernel. The evaluation of parameters indicated that it is insufficient to classify four species with only one and two parameters, but ten parameters were recommended in order to achieve satisfactory accuracy. The combination of different types of parameters, such as branch and crown parameters, can significantly improve classification accuracy. Finally, five sets of optimal parameters were suggested according to their importance and performance. This study also showed that the time- and cost-efficient HLS instrument could be a promising tool for tree-structure-related studies, such as structural parameter estimation, species classification, forest inventory, as well as sustainable tree management.

Keywords: structural properties; tropical species; handheld laser scanning; machine-learning classifiers; optimal parameter sets

Citation: Wang, M.; Wong, M.S.; Abbas, S. Tropical Species Classification with Structural Traits Using Handheld Laser Scanning Data. *Remote Sens.* **2022**, *14*, 1948. https://doi.org/10.3390/rs14081948

Academic Editors: Carlos Portillo-Quintero, José Luis Hernández-Stefanoni, Gabriela Reyes-Palomeque and Mukti Subedi

Received: 1 March 2022
Accepted: 11 April 2022
Published: 18 April 2022

1. Introduction

Urban trees play a vital role in ameliorating urban environment by reducing pollution [1], mitigating urban heat islands [2,3]. However, the degree of beneficence to environment is highly dependent on tree species [4]. The precise classification of tree species is thus necessary for better understanding our ecosystem services and developing strategies of urban sustainable development [5]. Recently, LiDAR technique, which uses pulsed laser to measure the physical attributes of object surface by calculating the distance between the objects and the laser sensor [6–9], is becoming increasingly popular in the forest research field as it can capture the tree structure information which is helpful for providing alternates for tree species classification [10–12]. According to the platform, the LiDAR technology includes spaceborne, airborne and terrestrial LiDAR [13]. Compared to spaceborne and airborne LiDAR, TLS offers a potential and efficient solution to acquire accurate structural information [14]. However, traditional TLS collects point cloud on

a static workstation, requiring much time for preparations and data preprocessing [13]. The HLS, equipped with lightweight laser scanner, could capture 3D data at a movable platform. The structural information and changes of trees in urban and rural areas can be easily and quickly acquired. For example, after typhoons or heavy rainstorms, HLS can help to rapidly obtain and evaluate the potential structural damage of trees. Several studies have verified that the point clouds captured by HLS was promising for basic tree structural properties estimation, i.e., tree height (TH), crown spread (CS) and diameter at the breast height (DBH) [15–17]. However, there is a lack of feasibility study on HLS for species classification. The tropical forests cover about 45% of the world's forest, comprising a highly diverse ecosystem [18]. Many studies in the literature studied tree species in tropical forests, and less focus has been paid to the classification of tropical tree species in urban areas. Therefore, to bridge the research gap, a study about classification of tropical species in a city using HLS was conducted.

Structural information of trees extracted from 3D point cloud is usually characterized as LiDAR parameters for species classification according to previous studies, such as explicit tree structure feature parameters [14], quantitative structural features [19] and salient geometric features [20]. However, most existing parameters were designed for the classification of boreal or temperate species and may not perform well on tropical species. To bridge the gap, we propose to explore appropriate structural parameters for tropical species classification and evaluate the effectiveness of these parameters extracted from HLS point cloud.

Therefore, in this study, a series of LiDAR structural parameters that could represent the differences between species were designed and extracted from individual tree point clouds obtained by HLS of four tropical species, including 6 branch parameters, 11 crown parameters and 6 entire tree parameters. Five ML models were developed for species classification, respectively. The importance of each parameter and the performance of different types of parameters were also evaluated, respectively. According to the classification results, we recommended several optimal parameter sets. The rest of this paper is organized as follows. Section 2 describes the research data collection and data processing. Section 3 introduces research methodologies, including separation of tree components, derivation of LiDAR structural parameters, classification of tropical species, as well as assessment of classification results. Section 4 describes all results, and Section 5 analyses the performance, influences, applicability, as well as potential improvements. Overall conclusions are summarized in Section 6.

2. Research Site and Data and Methods

2.1. Research Area and Tree Species

Hong Kong, which is located south of the Tropic of Cancer, has a humid subtropical climate. There were about 3300 species of plants [21], among which 12 species were noted as dominant tropical species according to the number of trees [21–23]. To select appropriate suitable species as research targets, we used three rationales: (1) tree shape. From the aspect of tree structures, tropical trees are mainly tall and top heavy [24,25], i.e., most of the leaves are at the top half of the tree. Thus, the crown length of selected species should be about or less than half of tree height; (2) tree number. To ensure the quality of the captured point cloud, the selected species needs to be sufficient so that enough target samples can be obtained; (3) tree location. The target individual trees should be able to be well separated for structural information extraction. Following these three rationales, four tropical species were finally selected, i.e., *Aleurites moluccana* (L.) Willd. (AM), *Ficus altissima* Blume (FA), *Delonix regia* (Boj. Ex Hook.) Raf. (DR) and *Hibiscus tiliaceus* L. (HT) [26].

Aleurites moluccana is native of Malaysia and Polynesia and widely cultivated in tropical and some subtropical areas [27]. It is an evergreen tree with wide spreading and large tree height. The leaves are simply and alternately arranged with entire and wave margins and 3–5 shallow lobes [28]. *Ficus altissima* native in southeastern Asia, and mainly distributes in Andam Islands, Myanmar and Malesia [29]. It is a large evergreen

tree with a spreading crown, often with aerial roots. The leaves are alternate, elliptic to ovate, with entire margins. *Delonix regia* is native of Madagascar and widely distributes in tropical and subtropical areas [30]. The leaf is even-bipinnately compound, and the canopy spread horizontally. *Hibiscus tiliaceus* is native of eastern hemisphere tropics [31]. Its leaves are heart shaped with finely serrated margins and the crown spread roundly with many branches. In these four species, two types of shape that are the common crown shape of tropical species [24,25] were included. AM and HT have a sphere-like crown with simple and complex structures, respectively, while FA and DR have a funnel-like crown with complex and simple structures, respectively. The trees of the selected species distribute in parks or along roadsides in the Kwun Tong district and Hong Kong Island (Figure 1). The basic structural information of trees used in this study was manually measured (Table 1). Figure 2 shows some examples of point cloud of selected four species.

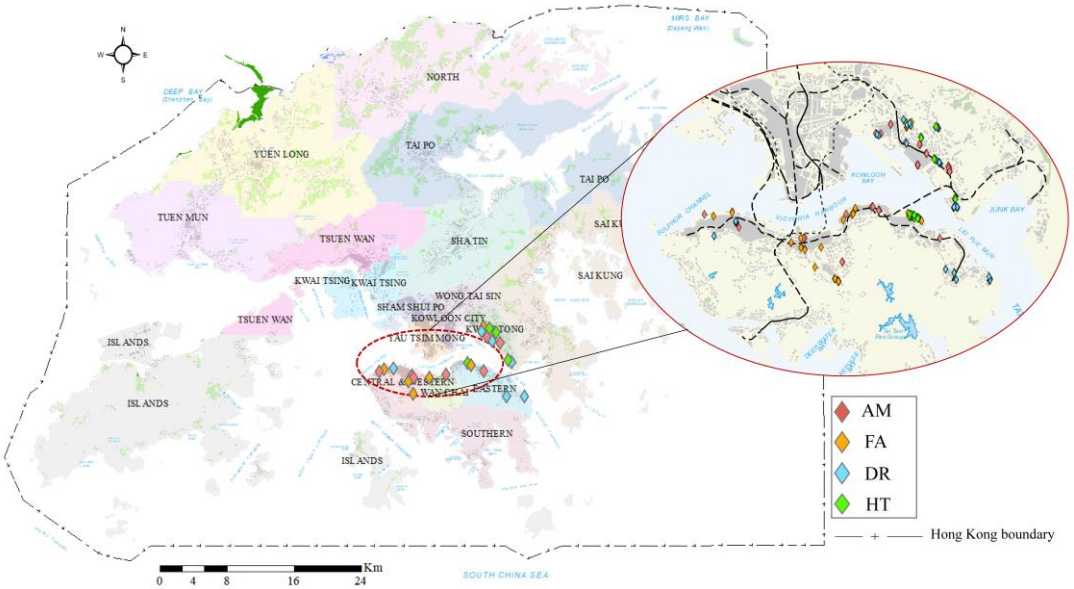

Figure 1. Location of research area and distribution of trees of selected four species. The colored icons in the dashed red circle indicate the general location of the selected four species. The icons in the solid red circle are specific sample locations of each species.

Table 1. Basic structural information of trees of four species. Mean, Max and Min are average, maximum and minimum values of TH, CS and DBH, respectively.

Species	Number	Structure Information			
			Mean	Max	Min
AM	63	TH (m)	13.27	21.27	7.458
		CS (m)	9.02	15.35	4.68
		DBH (cm)	35.29	58.92	21.38
FA	53	TH (m)	12.96	19.53	5.31
		CS (m)	10.79	18.72	4.74
		DBH (cm)	31.16	65.80	26.01
DR	52	TH (m)	10.76	18.33	5.84
		CS (m)	11.47	21.75	4.65
		DBH (cm)	23.86	30.44	13.61
HT	57	TH (m)	9.55	13.12	4.74
		CS (m)	7.37	13.71	3.48
		DBH (cm)	28.46	46.50	22.31

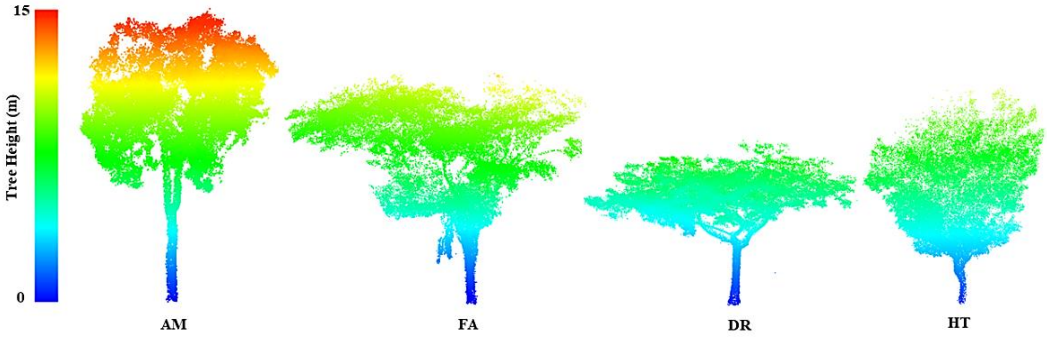

Figure 2. Examples of point cloud of four species. Four species from left to right are *Aleurites moluccana*, *Ficus altissima*, *Delonix regia* and *Hibiscus tiliaceus*, respectively.

2.2. Data Collection and Preprocessing

The mobile equipment used for data collection was a lightweight (3.5 kg) personal handheld laser scanner, ZEB HORIZON, developed by GeoSLAM Ltd. for outdoor use. This equipment incorporates a Velodyne Puck VLP-16 laser scanner that emits 937 points per scan line with 0.38° intervals at a wavelength of 903 nm (approximately 300,000 points per second). Its scanning range is up to 100 m. HLS point clouds of sample trees were collected during April and May of 2020, specifically, from 6 April to 29 May 2020. The scanning was conducted around trees in circles twice while walking at the speed of about 1.5 km/h. To ensure the scanning of structural information, we scanned the tree at a close distance (about 3 m) for the first circle and scanned the tree at a long distance (more than 10 m) for the second circle. For example, to the trees along the road, we firstly scanned the tree on the same roadside and secondly scanned the tree on the opposite roadside. The average scanning time for each tree was about 3–5 minutes.

Species classification was proposed to be conducted at the individual tree level in this study. Before the segmentation of individual trees, noise points were filtered out using the statistical outlier removal method, and ground points were removed by the cloth simulation filtering algorithm [32]. Both noise filtering and ground removal were implemented in CloudCompare 2.0 software. The individual tree point cloud was then initially segmented through marker-controlled watershed segmentation [32,33]. The markers were determined by the location of stems, which were detected through fitting cylinders with the least square algorithm at tree height of between 1.3 m and 1.4 m [34]. Manual refinement was subsequently executed on the initially segmented trees. Finally, the segmented individual trees of four species were preserved for later classification procedures.

3. Research Methodology

3.1. Separation of Tree Components

It is essential to separate the points into branch, stem and crown points before derivation of structural parameters. In this study, the leaves and wood points (including stems and branches) were first separated using a geometry-based algorithm that employs the shortest path detection method to separate the tree network. All points of a tree were regarded as nodes of the network. To each node, the neighbors were searched within a given number of steps. The more frequently a node was searched, the higher the possibility that a node could be a wood point. The conduction of leaf-wood separation was initially implemented using open-source python tool TLSeparation developed by Ref. [35]. Afterward, the refinement was manually implemented to recorrect the wrong separation.

Then, from the separated wood points, the branch and stem points were further classified based on the analysis of Euclidean distance *ed* [36]. The points whose *ed* between the neighbors was less than the restriction value ed_s were gathered into a small subset (a point can only belong to one subset). The certain restriction value and the number of neighbors were separately determined for each tree by experiments. Afterward, the

clustering procedure was conducted again on small subsets using a larger restriction value until all points were classified. In this way, the stem and branch points could be separated hierarchically. The conduction of separation of branch and stem points was implemented using MATLAB tools TreeQSM developed by Refs [19,37,38].

3.2. Derivation of Structural Parameters

From the aspect of plant physiology and plant morphology, it is insufficient to classify species based on one character, as each tree is a complex integrated system that includes stem, branch, root and leaves [39]. The characters should include characters of individual components and the whole tree [40,41]. Therefore, we proposed a series of structural characteristics and characterized them as 23 LiDAR parameters quantitatively (Table 2), involving parameters of individual components and parameters of the entire tree.

Table 2. The definition and formula of structural parameters.

Type	No.	Definition	Formula
Branch	B1	Stem branch angle	$B1 = \frac{1}{N_{B1}} \sum_{i=1}^{N_{B1}} A_i$
	B2	Stem branch cluster size	$B2 = \frac{1}{hl} \sum_{i=1}^{hl} B_{1\_hl_i}$
	B3	Stem branch radius	$B3 = \frac{1}{N_{B1}} \sum_{i=1}^{N_{B1}} \frac{SR_{i\_B1}}{TH}$
	B4	Stem branch length	$B4 = \frac{1}{N_{B1}} \sum_{i=1}^{N_{B1}} \frac{L_{i\_B1}}{TH}$
	B5	Stem branch distance	$B5 = \frac{1}{2B_1} \sum_{i=1,j=1}^{N_{B1}} d_{bi\_bj}$
	B6	Average of ratio between angles of first branches and second branches	$B6 = \frac{1}{N_{B1}+N_{B2}} \sum_{i=1}^{N_{B1}} \sum_{j=1}^{N_{B2}} A_{b1i\_b2j}$
Entire tree	T1	Ratio between DBH and tree height	$T1 = \frac{DBH}{TH}$
	T2	Ratio between DBH and tree volume	$T2 = \frac{DBH}{TV}$
	T3	Ratio between DBH and minimum stem radius	$T3 = \frac{DBH}{SR_{min}}$
	T4	Volume below 55% of the tree	$T4 = VC_{55}$
	T5	Cylinder length/tree volume	$T5 = \frac{l_c}{TV}$
	T6	Relative volume ratio	$T6 = \frac{VC_{80-90}}{VC_{0-10}}$
Crown	C1	Crown lowest heights/tree height	$C1 = \frac{CH_{l\_min}}{TH}$
	C2	Height difference between the start and end heights of a crown	$C2 = H - CH_{l\_min}$
	C3	Ratio between crown diameter and vertical height	$C3 = \frac{ed_{crown}}{C2}$
	C4	Ratio between minimum and maximum height of the crown bottom	$C4 = \frac{CH_{l_min}}{CH_{l_max}}$
	C5	Ratio between crown vertical length and tree height	$C5 = \frac{C2}{TH}$
	C6	Ratio between heights of the widest crown and the tree	$C6 = \frac{H_{spreadiest}}{TH}$
	C7	Ratio between crown cover area and tree height	$C7 = \frac{A_{xy}}{TH}$
	C8	Ratio between crown horizontal and vertical areas	$C8 = \frac{A_{xy}}{(A_{yz}+A_{xz})/2}$
	C9	Ratio between the maximum diameters of crown horizontal projection	$C9 = \frac{d_s}{d_c}$
	C10	Ratio between the maximum diameters of crown vertical projection	$C10 = \frac{d_{crown\_yz}}{d_{crown\_xz}}$
	C11	Ratio between heights of the crown and its widest part	$C11 = \frac{SH_{crown}}{H_{spreadiest}}$

Where N_{B1} is the number of first branches, A_i is the angle between branch and trunk, hl is the number of layers with a height of 0.4 m, $B_{1\_hl_i}$ is the number of first branches in the height layer i, SR_{i_B1} is the radius of stem at the height of first branch i, L_{i_B1} is the length of the first branch i, d_{bi_bj} is the vertical distance between the first branch bi and bj, A_{b1i_b2j}

is the angle between the first branch $b1i$ and second branch $b2j$, N_{B2} is the number of second branches, TV is tree volume, SR_{min} is the minimum stem radius, l_c is the total length of all cylinders, VC_{80-90} is the volume of cylinders with heights between 80–90%, VC_{0-10} is the volume of cylinders with heights between 0–10%, CH_{l_min} is the lowest height of the crown, ed_{crown} is the equal diameter of the crown, $H_{spreadiest}$ is the height of the widest crown spread, A_{xy} is the projection area of the entire crown onto the x–y plane, A_{yz} is the projection area of the entire crown onto the y–z plane, A_{xz} is the projection area of the entire crown onto the x–z plane, d_s is the maximum diameter of a crown, d_c is the maximum cross diameter of a crown, d_{crown_yz} is the maximum diameter of the crown projecting on the y–z plane, d_{crown_xz} is the maximum diameter of the crown projecting on the x–z plane, SH_{crown} is the crown start height.

Branch and entire tree parameters were extracted based on the 3D tree model TreeQSM developed by Refs [37,38]. The branch and stem points were first fitted by 3D cylinders using the least square algorithm. All cylinders were then integrated as the branch and stem model. The branch radius, branch length, branch angle, as well as DBH, could be extracted from the branch and stem model. The design of specific branch and stem parameters refer to Åkerblom et al. [19] and Terryn et al. [42]. Crown parameters were directly extracted from the tree point cloud. Among them, the derivation of C1–C3 refers to Ref. [14]. C4 reflected the flatness of the crown bottom and was calculated as the ratio between the minimum height CH_{l_min} and maximum height CH_{l_max} of the low crown. C6 was hierarchically computed with a layer height of 0.1 m referring to previous studies [14,38,43]. The spread area of each layer was calculated by the α-shape algorithm based on the projection of layer points on the x–y plane [44,45]. The ratio of the height with the largest projection area ($H_{spreadiest}$) to tree height was set as C6. C7 was defined as the projection area of the entire crown (projected onto the x–y plane), and C8 was the ratio of the crown projection area on the x–y plane to the average projection areas on the y–z and x–z planes. C9 was generated from the maximum diameters in two different directions (D_c and D_s; see Figure 3) of the crown projected onto the x–y plane. C10 was generated by averaging the ratios between the maximum diameter of the crown projected onto the y–z plane to that projected onto the x–z plane.

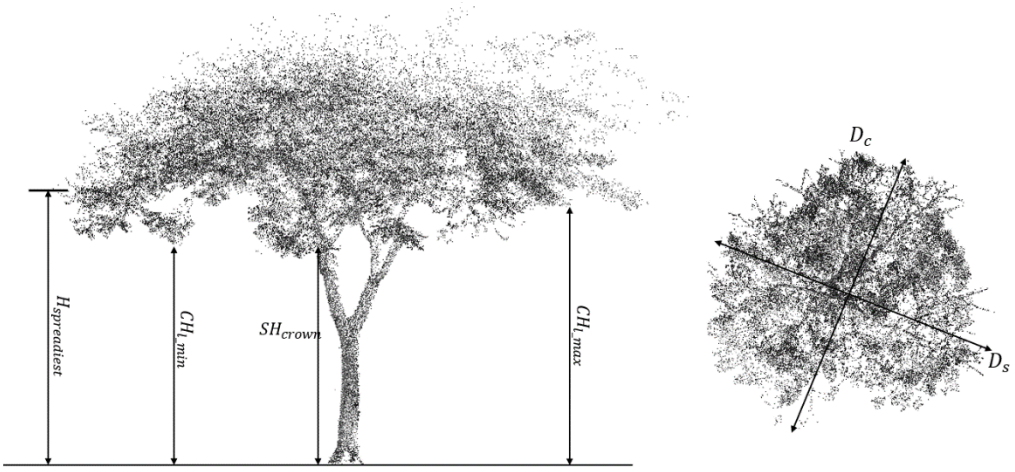

Figure 3. Illustration of crown parameters. $H_{spreadiest}$ is the height with the largest projection area. CH_{l_min} and CH_{l_max} are the minimum and maximum height of low crown, respectively. SH_{crown} is crown start height. D_s and D_c are the maximum crown spread and maximum crown cross-spread, respectively.

Parameters that differ significantly from each other usually perform better in classification problems than similar parameters [19]. Therefore, a correlation analysis between the parameters and the selection of appropriate parameters become important [46]. In this study, the Pearson correlation coefficient algorithm [47] was used to evaluate the relationship between all proposed parameters. The threshold 0.8 of correlation coefficient *r*value

was employed to differentiate high or low correlated parameters, i.e., the parameters whose $|r| > 0.8$ were regarded to have a high correlation.

3.3. Species Classification Approach

Various algorithms employed in previous studies of species classification generated various results [20,48]. For example, Xi et al. [49], Terryn et al. [42] and Åkerblom et al. [19] obtained classification accuracy of 87.9%, 79.29% and 82.0% using the K-nearest neighbor (KNN) algorithm and classification accuracy of 88.7%, 81.4% and 75.2% using the support vector machine (SVM) algorithm. In addition, these classification algorithms were implemented in different environments and were used to classify different species. Terryn et al. [42] and Åkerblom et al. [19] classify two understory and three temperate species, as well as three temperate species in mixed forests, respectively. Lin and Herold [14] classified four boreal species in the park with SVM and obtained robust accuracy of 77.5%. In this study, five ML algorithms were employed to classify four species, i.e., artificial neural network (ANN) [50], decision tree (DT) [51], KNN [52], random forest (RF) [53], SVM [54]. Three kernels of SVM (i.e., radial basis function kernel (SVMrbf) [55], polynomial kernel (SVMpoly) [55] and sigmoid kernel (SVMsig) [56,57] were evaluated separately because they map variables onto diverse spaces and can obtain different classification results [58]. The performance of the five ML models on tropical species classification was compared subsequently.

For the training and testing of ML models, 70% of trees of each species were randomly selected as the training dataset T composed of parameter–species pairs (xt, st), where $xt \in \mathbb{R}^M$ (M being the number of parameters) was a list of parameter values and $st \in Species = \{st_1, st_2, st_3, st_4\}$. The remaining 30% of trees were reserved as the testing dataset P. Each algorithm was trained with five-fold cross-validation. T was split into five parts, with one part being the validation data for turning the ML algorithm, and the remaining four parts being the training data (Figure 4). The algorithm was required to be trained and validated on all five folds, ensuring that all parts can be utilized as validation data. The species classification ability of the trained algorithms was tested by predicting the tree species in the testing dataset.

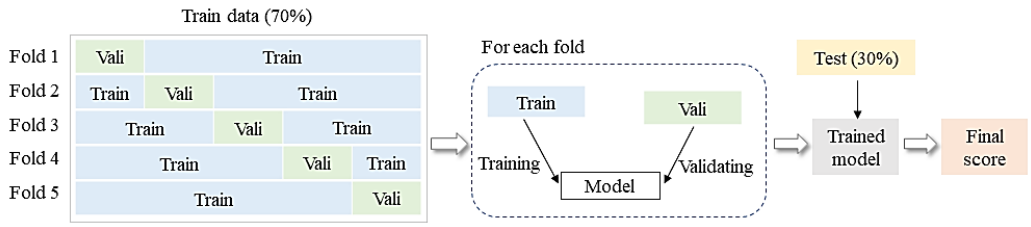

Figure 4. Workflow of the classification method. Vali in each fold of train data means validation data. The classification model is trained on the Train of each fold and is validated on Vali. After training on each fold, the parameter of the trained model is saved and used as the initial parameter of the classification model of next fold. The final trained model is evaluated using Test (30%).

Previous studies demonstrated that parameter sets that contain various types and numbers of parameters produce different classification results [14]. For example, Othmani et al. [59] obtained classification accuracy of 80.62% using three stem geometric texture features. Lin and Herold [14] employed 10 explicit structural features to classify four species and gained a classification accuracy of 77.5%. Wei et al. [43] achieved classification accuracy of 71.93% using 14 stem-related feature parameters. To explore the effectiveness of the parameter sets, the classification model was implemented with individual parameters and parameter sets with counts ranging from 1 to 21, respectively. All combinations of parameters were evaluated in this study. For example, when the parameter count was one, the species were classified using one parameter. When the parameter count equaled two, the species were classified using two parameters (all combinations of two parameters were tested).

3.4. Assessment of Classification Results and Structural Parameters Importance

Assuming that frequently appearing parameters in parameter sets used for species classification play a more significant role than low-frequency parameters, we evaluated the importance of each parameter through the following steps: (i) filter out the top 200 parameter sets with the highest W_{ac} and measure the frequency of each parameter; (ii) the ratio of the frequency to 200 is regarded as the importance value of each parameter; the higher the ratio, the more important the parameter. The more important the parameter, the closer to 1 the importance value.

To reduce the influence of unbalanced datasets on classification results, the general classification performances of the ML algorithms for the four tree species were evaluated based on their weighted-average accuracies (W_{ac}). The ratio of the sample count in each species to the total number of samples was regarded as their corresponding weights. Then, W_{ac} was generated by summing the weighted accuracies of each species as

$$W_{ac} = \frac{N_{AM}}{N} \times AC_{AM} + \frac{N_{FA}}{N} \times AC_{FA} + \frac{N_{DR}}{N} \times AC_{DR} + \frac{N_{HT}}{N} \times AC_{HT}, \quad (1)$$

where N denotes the total number of trees, and N_{AM}, N_{FA}, N_{DR} and N_{HT} indicate the number of trees of species AM, FA, DR and HT, respectively. AC_{AM}, AC_{FA}, AC_{DR}, AC_{HT} denote the accuracy of each species.

For specific species, the performances of the ML algorithms were measured based on their user accuracies (AC). For each species, AC was calculated as the ratio of the number of correct classifications to the number of all trees of the corresponding species. For example, the AC value of species AM (AC_{AM}) was calculated as

$$AC_{AM} = \frac{N_{c\_AM}}{N_{AM}}, \quad (2)$$

where N_{c_AM} is the number of correctly classified AM trees, and N_{AM} is the total number of AM trees.

4. Results

4.1. Derived Structural Parameters

To evaluate the capability and effectiveness of HLS for structural parameter derivation, the basic tree structural information extracted from HLS data was compared with field-measured values (Figure 5). The results showed that the errors of tree height and crown spread of four species between field-measured and extracted parameters are small, but DBH has relatively large biases, especially the DBH of FA. This may be because some aerial root points of FA were wrongly classified as stem points, thus increasing the differences.

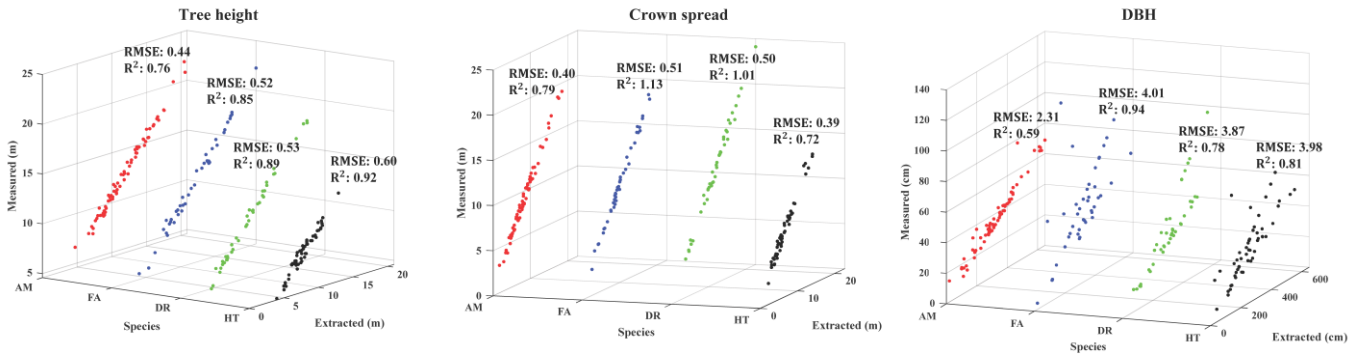

Figure 5. Comparison of tree basic parameters of four species between manual measured values and extracted values from 3D tree model. RMSE and R^2 are the root mean squared error and r-squared error of each parameter.

A large diversity between species can be observed (Figure 6), for example, the value range of parameter C1 is significantly different between AM and HT. B5 can split AM and FA but is of limited use for the separation of DR and HT. Similarly, C8 can split FA and DR, but it could not be used for the separation of AM and HT. This also demonstrates that one parameter is hard to classify all four species. This is consistent with the illustration of Refs [40,41] that it is difficult to identify tree species according to individual characters.

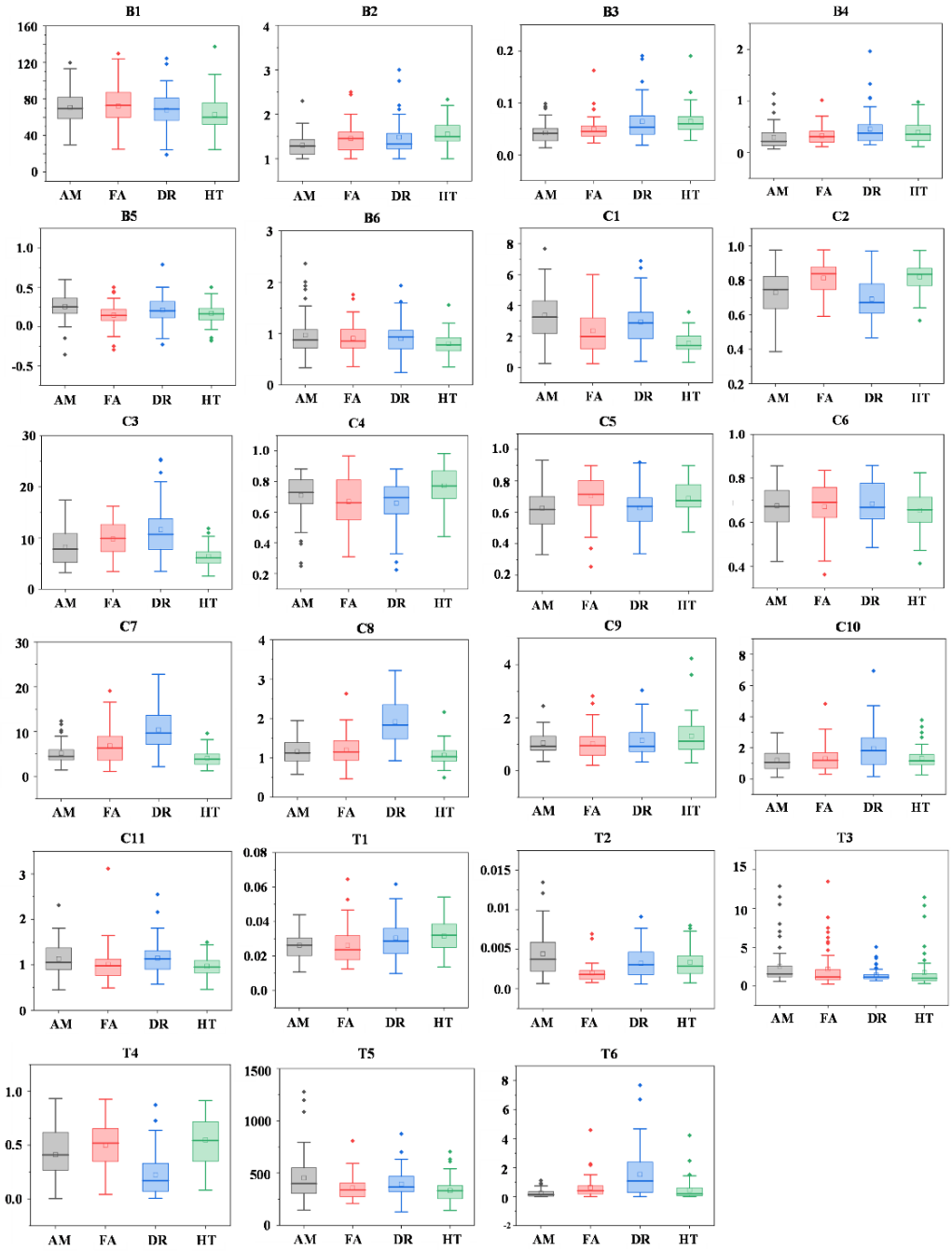

Figure 6. Boxplot of all structural parameter values of four selected species. The individual points out of the box are the outliers of each parameter of each species. The horizontal lines below and above the box are the minimum and maximum values excluding outliers, respectively. The bottom line and top line of the box are the median values of the lower half and upper half of the parameter of each species, respectively. The bold line and square in each box are the median and mean value of each parameter of each species, respectively.

However, when taking the crown shape and structural complexity into consideration, the performance of individual parameters can be grouped. In this study, AM and HT are species that have the sphere-like crown with a simple and complex structure, respectively, while DR and FA are species that have the funnel-like crown with simple and complex structures, respectively. From the aspect of the crown shape, to the sphere-like and funnel-like crown with simple structure, C7, C8, T3, T4, T6 can classify most trees of AM and DR, and with the sphere-like and funnel-like crown with complex structure, B3, C3, C7, T2 perform better. From the aspect of structural complexity, B2, B3, B5, C1, C3, C5, C7, T3 show great ability in distinguishing trees that have the sphere-like crown with simple or complex structures, and to trees that have the funnel-like crown with simple or complex structures, C2, C5, C8, T4 perform better in distinguishing the species.

4.2. Correlations Analysis Results

In three types of parameters, the branch parameters have relatively lower correlation coefficients with crown and entire tree parameters. In six branch parameters, B1 and B6 have relatively higher correlation coefficients. The rest $|r|$ values are all smaller than 0.5. Compared with branch parameters, crown parameters have higher correlation coefficient values. Ten $|r|$ values are higher than 0.5, i.e., C1 and C2, C2 and T4, C3 and C7, C3 and T2, C4 and C5, C5 and T4, C5 and C11, C6 and C11, C7 and C8, C8 and C10, C11 and T4. The entire tree parameters have higher correlation coefficient values with crown parameters than with branch parameters.

For individual parameters, most of the parameters were weakly related to each other, except for two pairs (Figure 7): C1 and C2, as well as C5 and C11. Significantly strong negative relationships were observed between these two pairs (r value between C1 and C2 is equal to -0.8 and that between C5 and C11 is -0.85). In addition, r values between these four parameters and other parameters were considered for parameter selection. C2 and T2 had a moderately high positive relationship with an r value of 0.6, and C11 and C6 had an r value of 0.68. Compared with C2 and C11, C5 and C1 had lower relationships with other features. Therefore, C2 and C11 were filtered. A total of 21 parameters finally remained for the classification of four species: B1–B6, C1, C3–C10 and T1–T6.

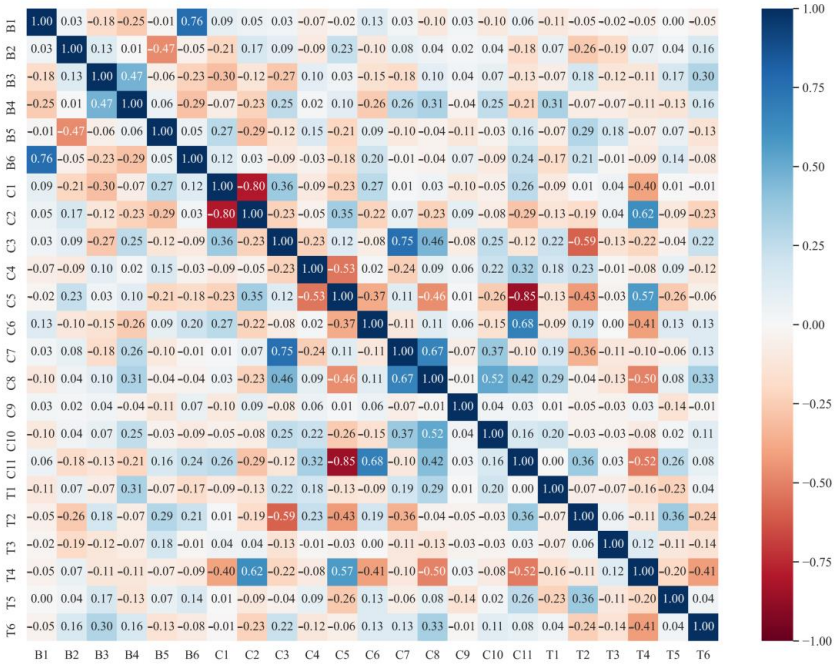

Figure 7. Correlation coefficient (r) values between proposed structural parameters. The darker the blue color, the higher positive the correlation between structural parameters. The darker the red color, the higher negative the correlation between structural parameters.

4.3. Species Classification Results

4.3.1. Ability of Single Parameters for Species Classification

From the classification results, we can further observe the ability of individual parameters in tropical species classification. The univariate analysis indicated that two or three species can be separated by some proposed structural parameters, but it was difficult for each parameter to distinguish all species effectively (Table 3). W_{ac} values of structural parameters varied from 19.7% to 45.45%. This is consistent with our analysis of derived structural parameters in Section 4.1. The low capacity of individual parameters for the classification of four species has also been verified in previous research [60–62]. Besides, the performance on crown shape and structural complexity was similar with above analysis. For example, C8 was sensitive to the structural complexity between sphere-like crown and the crown shape with complex structure; the classification accuracy of DR using C8 was the highest. C3 was sensitive to the crown shape with complex structure and the structural complexity of the crown shape; the classification accuracy of HT using C3 was the highest.

Table 3. Overall weighted accuracy (W_{ac}) of four species using each parameter and the classification accuracy of four species (AC_{AM}, AC_{FA}, AC_{DR}, AC_{HT}) using each parameter. Par indicates the name of structural parameters. Type demonstrates the group of structural parameters.

Type	Par	AC_{AM}	AC_{FA}	AC_{DR}	AC_{HT}	W_{ac}
Branch	B1	28.57	42.31	41.67	35.71	37.88
	B2	7.14	30.43	41.94	66.67	36.36
	B3	18.18	50.00	15.79	8.33	27.27
	B4	23.08	26.67	40.00	16.67	27.27
	B5	40.00	28.57	30.00	26.67	30.30
	B6	33.33	22.73	17.65	13.33	21.21
	Average	25.05	25.05	31.17	27.89	30.04
Crown	C1	26.67	9.09	47.37	20.00	25.76
	C3	42.86	47.06	43.75	47.37	45.45
	C4	20.00	20.00	23.81	50.00	25.76
	C5	33.33	35.29	27.27	26.67	30.30
	C6	7.14	25.00	26.09	26.67	22.73
	C7	35.71	33.33	31.25	28.57	31.82
	C8	11.76	30.00	57.89	45.00	37.88
	C9	22.22	27.27	5.56	23.53	19.70
	C10	33.33	47.06	32.00	20.00	33.33
	C11	34.21	33.33	40.31	29.57	36.18
	Average	26.72	30.74	33.53	31.74	30.89
Entire tree	T1	50.00	10.53	22.22	35.29	27.27
	T2	25.00	57.14	13.33	11.11	28.79
	T3	20.00	38.46	32.00	27.78	30.30
	T4	22.22	16.67	45.00	21.05	27.27
	T5	33.33	35.00	27.78	12.50	27.27
	T6	43.75	26.67	40.00	35.00	36.36
	Average	32.38	30.75	30.05	23.78	29.54

Furthermore, the classification accuracy also shows the ability of each parameter. In all parameters, C3 shows the best performance with the highest weighted accuracy W_{ac} of 45%. To distinguish crown shape and structural complexity, T6, B1 and B2, T1 and T6, C8 indicate great ability in the identification of crown shape with a simple structure, crown shape with a complex structure, structural complexity of sphere-like crown, structural complexity of funnel-like crown, respectively. It is also noted that the performance of individual parameters on specific species varied dramatically. For instance, B1 and B2 both have great performance in the identification of the crown shape with a complex structure, but B1 prefer FA, while B2 prefer HT.

As observed from the average weighted accuracy, the ability to distinguish four species of crown parameters is slightly higher than branch parameters. Entire tree parameters have the lowest distinguishing ability. From the average classification accuracy of four species, the species with sphere-like crown, branch and crown parameters have better ability in distinguishing complex structure than simple structure, while entire tree parameters have better ability in distinguishing simple structure. In contrast with species with the funnel-like crown, branch and crown parameters have a better ability in distinguishing simple structure than complex structure, while entire tree parameters have a better ability in distinguishing the complex structure.

4.3.2. Ability of Parameter Sets in Species Classification

Combining parameters of the same type achieved a relatively lower accuracy (Table 4). Among the three types, structural parameters representing the branch characteristics showed the smallest power in species classification. Crown and entire tree parameters had similar classification accuracy (W_{ac} of the combined crown parameters was slightly larger than the combined entire tree parameters). The combination of two types of parameters significantly improved the classification results. Among them, the combination of crown and entire tree parameters achieved excellent performance, with an overall accuracy of up to 80.64%. The highest accuracy (84.09%) was achieved by integrating the parameters of all three types.

Table 4. Overall weighted accuracy of four species achieved using all structural parameters in each group, each two groups and all three groups, respectively.

Branch	Crown	Entire Tree	W_{ac}
√			57.86
	√		61.27
		√	60.34
√	√		73.14
√		√	79.59
	√	√	80.64
√	√	√	84.09

In five classification models, the SVM classifier obtained generally better classification results, and the SVMpoly classifier achieved the highest W_{ac} value of 84.09% (Table 5). This may be because compared with other classifiers, SVM is better at dealing with classification problems with a small sample size [63]. The *AC* values of AM and DR achieved by all classification algorithms were higher than those of FA and HT, indicating that the structures of AM and DR were more easily identified than those of FA and HT. A possible explanation is that the complexity of structures of AM and DR is less than FA and HT from the aspect of plant morphology. The performance of the other two kernels of SVM classification was more unstable. Although all AM trees were correctly identified by SVMrbf and SVMsig, the classification abilities of these two classifiers with the other three species were seriously imbalanced. To understand the classification ability of the employed structural parameters for each species, we listed the number of correctly classified trees of each species (Table 6). As seen in the table, about 75% of the incorrectly classified FA trees were identified as HT, and half of the incorrectly classified HT trees were identified as FA. This may be because the crowns of HT and FA are both funnel shape, resulting in similar ranges of many of their structural parameters.

Table 5. Overall weighted accuracy of four species and the classification accuracy of each species achieved by all classification models.

Classification Results	ANN	DT	KNN	RF	SVMpoly	SVMrbf	SVMsig
AC_{AM}	78.57	58.82	80.00	90.00	92.86	100.00	100.00
AC_{FA}	66.67	68.42	63.16	66.67	72.22	61.90	63.64
AC_{DR}	90.48	70.00	88.89	78.95	89.48	78.89	85.00
AC_{HT}	62.50	80.00	57.89	68.75	73.33	61.90	70.59
W_{ac}	75.10	69.47	72.94	75.63	84.09	77.75	79.08

Table 6. Confusion matrix of classification results with the highest weighted accuracy. The value indicates the ratio of samples that were correctly predicted to reference samples.

		Prediction				
		AM	**FA**	**DR**	**HT**	**Total**
Reference	AM	58.82	80.00	90.00	92.86	100.00
	FA	68.42	63.16	66.67	72.22	61.90
	DR	70.00	88.89	78.95	89.48	78.89
	HT	80.00	57.89	68.75	73.33	61.90
	Total	69.47	72.94	75.63	84.09	77.75

Furthermore, we discussed the effect of varying the parameter counts for tropical species classification using HLS point clouds. A gradual improvement in classification accuracy can be observed with the increase in parameters (Figure 8). The highest classification accuracy was achieved when 10 parameters were fed into the classifiers. Subsequently, the classification accuracy steadily decreased with increasing parameter counts, demonstrating that including more parameters does not necessarily lead to better classification. The appropriate number of structural parameters may be about 10 for tropical species classification.

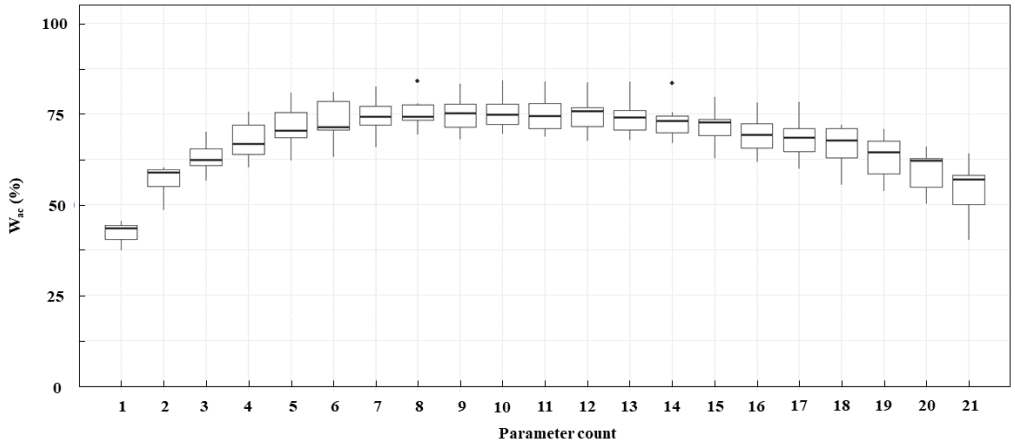

Figure 8. Boxplot of overall weighted accuracy achieved by all classification models using different number of structural parameters. The bold line means the median value of all weighted accuracy achieved by the corresponding number of parameters. The individual black points are the outliers of all weighted accuracy. The bottom line and top line of the box are the median of lower half and upper half of all weighted accuracy achieved by the corresponding number of parameters.

4.4. Optimal Parameter Sets

Among 21 parameters, 8 have importance values exceeding 0.5 (Figure 9), involving 3 branch parameters (B3, B5, and B6), 2 crown parameters (C1 and C4) and 3 entire tree parameters (T3, T4 and T6). The most important parameter was T3 (with an importance value close to 1), followed by C4 and T6 with importance values of approximately 0.75. The

changing trend of the stem radius of our four species is the opposite. As seen in Figure 2, the stem of AM and DR grows straightly, and the stem becomes thinner as the tree grows taller. However, the aerial root points of FA were likely to be misclassified as stem points, leading to the stem radius becoming larger as the tree grows. This may be the reason why T3 plays the most important role in species classification. C4 reflects the flatness of the crown bottom; it is also an illustration of the crown shape. The four species have four different crown shapes. T6 reflects the tree shape using the volume ratio of the crown top and stem. Taking DR and HT as examples, when they have similar stem radius, the crown top of DR has a larger volume than HT, as its crown spread is larger than HT. Correspondingly, T6 values of DR tend to be smaller than HT. The three important branch parameters mainly describe the properties of angle, interval and radius of first branches. These three parameters have been confirmed and applied in many previous studies [19,42,43,49,64]. Five optimal parameter sets were finally suggested based on the important assessment and classification results (Table 7). The classification accuracies achieved with these optimal parameter sets were also listed in the table. The W_{ac} values ranged from 83.70% to 84.09%. The best parameter set, which had the highest accuracy value, was composed of three branches, three crowns and four entire tree parameters, agreeing with the illustration mentioned in the above section that integrates all three types of parameters to obtain the best result.

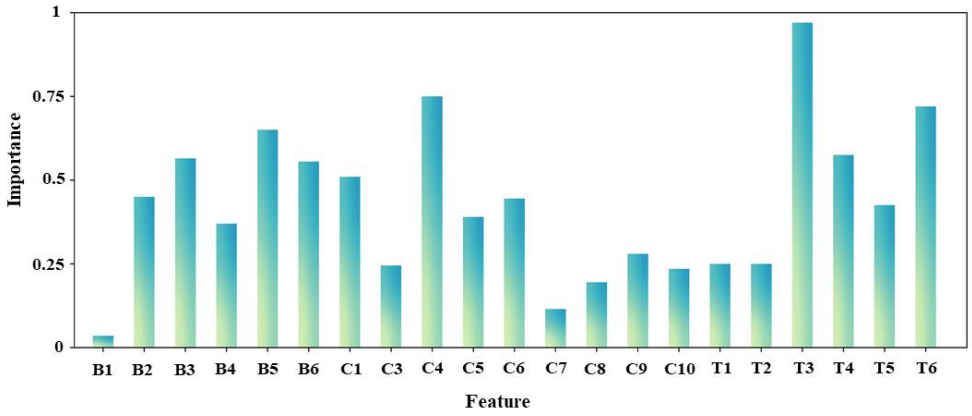

Figure 9. Importance values of employed parameters calculated from the top 200 weighted accuracies. The more frequently the parameter occurs in the first 200 parameter sets, the more important the parameter is, and the closer to 1 the importance value is.

Table 7. The overall weighted accuracy (W_{ac}) and classification accuracy of each species (AC_{AM}, AC_{FA}, AC_{DR}, AC_{HT}) achieved by optimal structural parameter sets using the best classification model.

Optimal Parameter Sets	AC_{AM}	AC_{FA}	AC_{DR}	AC_{HT}	W_{ac}
B3, B5, B6, C4, C5, C6, T3, T4, T5, T6	92.86	72.22	89.48	73.33	84.09
B3, B6, T1, T2, T3, T4, C7, C8	90.48	70.67	88.89	72.73	83.96
B6, C1, C3, C4, C5, C6, C8, T1, T2, T3, T4	90.48	66.67	88.89	70.59	83.83
B2, B4, B6, C4, C7, T1, T2, T3	90.00	66.67	85.00	70.59	83.70
B2, B3, B5, C3, C5, C7, C10, T1, T2, T3, T4, T5, T6	90.00	68.42	85.00	68.75	83.70

5. Discussion

5.1. Influences and Limitations

Although positive classification results were obtained, there are some limitations in this study. Four tropical species employed in this study have the sphere-like or the funnel-like crown with different structural complexity. Although many tropical species have these two crown shapes [24,25], a number of natural and human factors can affect the crown shape and structural complexity. This means that there may be limitations when applying the proposed method on other crown shapes or species in the forests.

Tree samples used in this study were in the park or along the roadsides. The structural properties of other trees in the surroundings may be similar. Some trees can optimize their traits during growth to face the light in local conditions, resulting in neighborhood-induced convergence cross-species [65]. The structural features of these trees thus differ from the common structural pattern [66–69], affecting the accurate expression of LiDAR parameters for structural characteristics. Another influence is that the internal structures, such as small branches between leaves, are difficult to capture by LiDAR techniques, either HLS or TLS, resulting in few differences in internal structures between the species. LiDAR technique catches the 3D information of objects by emitting pulsed lasers to objects and receiving returned lasers from objects. The information on small branches that are covered by leaves cannot be captured by LiDAR.

The performance of the separation approach for tree components also impacts the parameter extraction and classification results. The structures of AM and DR are relatively simple, and their branch, stem and crown points can be identified more easily. As a result, the branch points separated from a tree point cloud may be more accurate, and the corresponding branch parameters can represent the structural difference more precisely. However, it is a little bit difficult to completely split the components of FA and HT. Some FA trees had aerial roots that developed from branches, affecting the identification of branch points and extraction of branch parameters. The branches of HT were usually covered by its broad leaves, leading to difficulty in capturing the detailed structures and inaccurate parameter extraction.

5.2. Applicability Analysis

With high flexibility and properties of acquiring data remotely, the HLS technique may not only be suitable for capturing tree structural information but also appropriate for forest biomass assessment, forest structure transformation, as well as forest inventory and management. Specifically, HLS, which provides a competitive approach for precise structural parameter estimation, can improve the accuracy of forest biomass mapping and forest inventory evaluation via effectively capturing complete individual tree point clouds. The change of basic structural parameters caused by storms, snow, drought or insect hazards can thus be detected without contact using HLS, which not only reduces the possibility of secondary damage to trees but also protects the safety of surveying workers. The proposed structural parameters may be employed as indices to measure damage by comparing the difference in structures before and after natural disasters, such as changes in first-order branch angles and branch length, reduction in crown size, crown volume and crown length, as well as variation of stem leaning degree. Trees in Hong Kong usually suffer typhoons. It is essential to explore the impacts of typhoons and evaluate the ability of trees to resist wind, especially valuable trees, such as old trees and stonewall trees. In addition, the relationship between the surrounding environments and tree structures can be explored through studying the changes in these parameters.

The proposed structural parameters that were proved to be effective for representing differences in structural characteristics between four tropical species can also provide an important reference for the classification of other species. Our structural parameters and corresponding classification results can be good references and resource materials for the classification of more tropical species. Additionally, these parameters were considered to be built as a library for species classification. In this way, the importance of structural parameters for different species is able to be ranked easily.

5.3. Potential Improvements

Four tropical species were researched as examples, which may lead to potential instability and uncertainty during the widely practical application of proposed parameters in the classification of other species. Therefore, in the future, we will include more species to further explore the potential of the proposed approach in the field of tropical species classification. Considering some restrictions may appear when classifying trees growing in

seriously crowded forests due to different environments, more samples of each species in diverse neighboring environments are expected to be included to minimize the influence of neighborhood-induced convergence, such as crowded or sparse road-side plots, single-species or mixed-species plots, urban forest or suburban forest.

The satisfactory classification results suggest that HLS is a promising tool for species classification in urban areas. Given its flexibility, HLS can detect more details of trees, thus boosting the species separation with the extracted features. Nevertheless, to achieve better results, the combination of HLS data and other remote sensing sources, such as multispectral or hyperspectral images, is worth consideration. Spectral information is a robust tool for species recognition, as proven by Ref. [70]. The combination of structural and spectral features is potentially an excellent approach and is worthy of our further focus in the future. The combination of HLS data and UAV LiDAR point cloud is also worth considering for achieving better results. UAV LiDAR can provide dense point clouds of the upper crown at low costs, and HLS can provide an extensive point cloud on the ground level. Based on further exploration, a 3D point cloud library of tropical species, containing species information, various structural parameters, as well as growth environment conditions, is proposed to be developed for later research. This library will provide references for quick species classification.

6. Conclusions

In this study, we proposed 23 structural parameters that represent structural properties from HLS individual tree point clouds for tropical species classification. Five classification models were employed to classify trees of the four species growing in urban areas. In addition, the performance of each parameter and optimal parameter sets were evaluated. The validation of basic parameters between the derived and manually measured data demonstrates that the structural information of trees can be accurately captured by HLS in a time- and cost-saving way. The comparison between the classification results of five models reveals that SVM is more suitable for parameter-based tropical species classification, and the highest accuracy of 84.09% is achieved by SVM with a polynomial kernel. Besides, the classification results affected by tree structure, generally, species with relatively simple structures have higher classification accuracy.

The investigation of the optimal parameter sets reveals that including all three types of structural parameters (i.e., branch, crown and entire tree parameters) can achieve higher accuracy than using single parameters or a single type of parameter. When optimizing the parameter count, it was also found that (a) including more parameters does not always provide better results and (b) a set of 10 parameters (three branch, three crown and four entire tree parameters) yielded the best results.

In summary, HLS was verified as a promising alternative to traditional static TLS for species classification. Our proposed parameters can effectively classify the four tropical species, providing an important reference for species mapping based on HLS technology. In future work, the application of the proposed parameters to classification tasks that involve more tree species, such as boreal and temperate species, will be further explored. Besides, a tropical tree point cloud library can be built using captured data for other research of all institutions in the world.

Author Contributions: Conceptualization, M.S.W.; methodology, M.S.W. and M.W.; validation, M.W.; formal analysis and investigation, M.W. and S.A.; writing—original draft preparation, M.W.; writing—review and editing, M.S.W. and S.A.; visualization, M.W. All authors have read and agreed to the published version of the manuscript.

Funding: This research was funded by the Research Institute of Land and Space and the PhD fellowship from the Hong Kong Polytechnic University, as well as the Research Grants Council, Hong Kong, China.

Institutional Review Board Statement: Not applicable.

Informed Consent Statement: Not applicable.

Data Availability Statement: Data available on request due to restrictions of privacy.

Acknowledgments: The authors would like to thank for the research funding (project: 1-CD81) supported by the Research Institute of Land and Space, the Hong Kong Polytechnic University and the PhD fellowship from the Hong Kong Polytechnic University. M.S. Wong thanks the funding support from General Research Fund (Grant No. 15602619 and 15603920), and Collaborative Research Fund (Grant No. C7064-18GF, C4023-20GF), from the Hong Kong Research Grants Council, Hong Kong, China. We also express our gratitude to the anonymous reviewers and the editor for their valuable comments and suggestions to improve the manuscript.

Conflicts of Interest: The authors declare no conflict of interest. The funders had no role in the design of the study; in the collection, analyses, or interpretation of data; in the writing of the manuscript, or in the decision to publish the results.

References

1. Chai, Y.; Zhu, N.; Han, H. Dust removal effect of urban tree species in Harbin. *Ying Yong Sheng Tai Xue Bao J. Appl. Ecol.* **2002**, *13*, 1121–1126.
2. Rahman, M.A.; Armson, D.; Ennos, A.R. A comparison of the growth and cooling effectiveness of five commonly planted urban tree species. *Urban. Ecosyst.* **2015**, *18*, 371–389. [CrossRef]
3. Wong, M.S.; Nichol, J.; Kwok, K.H. The urban heat island in Hong Kong: Causative factors and scenario analysis. In Proceedings of the 2009 Joint Urban Remote Sensing Event, Shanghai, China, 20–22 May 2009.
4. Alonzo, M.; Bookhagen, B.; Roberts, D.A. Urban tree species mapping using hyperspectral and lidar data fusion. *Remote Sens. Environ.* **2014**, *148*, 70–83. [CrossRef]
5. Pu, R.; Landry, S. A comparative analysis of high spatial resolution IKONOS and WorldView-2 imagery for mapping urban tree species. *Remote Sens. Environ.* **2012**, *124*, 516–533. [CrossRef]
6. Collis, R. Lidar. *Appl. Optics.* **1970**, *9*, 1782–1788. [CrossRef] [PubMed]
7. Dong, P.; Chen, Q. *LiDAR Remote Sensing and Applications*; CRC Press: Boca Raton, FL, USA, 2017; pp. 60–108.
8. Dubayah, R.O.; Drake, J.B. Lidar remote sensing for forestry. *J. Forest.* **2000**, *98*, 44–46.
9. Lim, K.; Treitz, P.; Wulder, M.; St-Onge, B.; Flood, M. LiDAR remote sensing of forest structure. *Prog Phys. Geog.* **2003**, *27*, 88–106. [CrossRef]
10. Guo, Q.; Liu, J.; Tao, S.; Xue, B.; Li, L.; Xu, G.; Li, W.; Wu, G.; Li, Y.; Chen, L.; et al. Perspectives and prospects of LiDAR in forest ecosystem monitoring and modeling. *Chin. Sci. Bull.* **2014**, *59*, 459–478.
11. Silva, C.; Hudak, A.; Rowell, E.; Seielstad, C.; Klauberg, C.; Bright, B.; Loudermilk, E.L.; O'Brien, J.J. Comparison of terrestrial and airborne LiDAR derived crown metrics for describing forest structure at Eglin Air Force Base, Florida, USA. In Proceedings of the 2017 ESA Annual Meeting, Portland, OR, USA, 6–11 August 2017.
12. Tao, S.; Labrière, N.; Calders, K.; Fischer, F.J.; Rau, E.P.; Plaisance, L.; Chave, J. Mapping tropical forest trees across large areas with lightweight cost-effective terrestrial laser scanning. *Ann. Forest Sci.* **2021**, *78*, 103. [CrossRef]
13. Bauwens, S.; Bartholomeus, H.; Calders, K.; Lejeune, P. Forest inventory with terrestrial LiDAR: A comparison of static and hand-held mobile laser scanning. *Forests* **2016**, *7*, 127. [CrossRef]
14. Lin, Y.; Herold, M. Tree species classification based on explicit tree structure feature parameters derived from static terrestrial laser scanning data. *Agric. For. Meteorol.* **2016**, *216*, 105–114. [CrossRef]
15. Ryding, J.; Williams, E.; Smith, M.J.; Eichhorn, M.P. Assessing handheld mobile laser scanners for forest surveys. *Remote Sens.* **2015**, *7*, 1095–1111. [CrossRef]
16. Stal, C.; Verbeurgt, J.; Sloover, L.D.; Wulf, A.D. Assessment of handheld mobile terrestrial laser scanning for estimating tree parameters. *J. For. Res.* **2020**, *32*, 1503–1513. [CrossRef]
17. Vatandaşlar, C.; Zeybek, M. Application of handheld laser scanning technology for forest inventory purposes in the NE Turkey. *Turk. J. Agri. For.* **2020**, *44*, 229–242. [CrossRef]
18. Lindquist, E.J.; D'Annunzio, R.; Gerrand, A.; MacDicken, K.; Achard, F.; Beuchle, R.; Brink, A.; Eva, H.D.; Mayaux, P.; San-Miguel-Ayanz, J.; et al. *Global Forest Land-Use Change 1990–2005*; Food and Agriculture Organization of the United Nations (FAO): Rome, Italy, 2012; p. 169.
19. Åkerblom, M.; Raumonen, P.; Mäkipää, R.; Kaasalainen, M. Automatic tree species recognition with quantitative structure models. *Remote Sens. Environ.* **2017**, *191*, 1–12. [CrossRef]
20. Yao, W.; Krzystek, P.; Heurich, M. Tree species classification and estimation of stem volume and DBH based on single tree extraction by exploiting airborne full-waveform LiDAR data. *Remote Sens. Environ.* **2012**, *123*, 368–380. [CrossRef]
21. Gov, H.K. The Natural Environment, Plants & Animals in Hong Kong. Nature Conservation. November 2021. Available online: https://www.gov.hk/en/residents/environment/conservation/naturalenvplantsanimals.htm (accessed on 22 January 2022).
22. Jim, C. Roadside trees in urban Hong Kong: Part II species coomposition. *Arboric J.* **1996**, *20*, 279–298. [CrossRef]
23. Jim, C. Tree–habitat relationships in urban Hong Kong. *Environ. Conserv.* **1992**, *19*, 209–218. [CrossRef]
24. Kuuluvainen, T. Tree architectures adapted to efficient light utilization: Is there a basis for latitudinal gradients? *Oikos* **1992**, *65*, 275–284. [CrossRef]

25. Lindh, M.; Falster, D.S.; Zhang, L.; Dieckmann, U.; Brännström, Å. Latitudinal effects on crown shape evolution. *Ecol. Evol.* **2018**, *8*, 8149–8158. [CrossRef]
26. Barrie, F.R.; Buck, W.R.; Demoulin, V.; Greuter, W.; Hawksworth, D.L.; Herendeen, P.S.; Knapp, S.; Marhold, K.; Prado, J.; Prudhomme, V.R.W.F.; et al. *International Code of Nomenclature for Algae, Fungi and Plants (Melbourne Code)*; Koeltz Scientific Books: Königstein, Germany, 2012.
27. Howes, F.N. *Nuts, Their Production and Everyday Uses*; Faber and Faber: London, UK, 1948.
28. Cooper, W.; Cooper, W.T. *Fruits of the Australian Tropical Rainforest*; Nokomis Editions: Buxton, Australia, 2004.
29. Nadel, H.; Frank, J.H.; Knight, J.R. Escapees and accomplices: The naturalization of exotic Ficus and their associated faunas in Florida. *Fla Entomol.* **1992**, *75*, 29–38. [CrossRef]
30. Dressler, S.; Schmidt, M.; Zizka, G. Introducing African Plants—A photo guide—An interactive photo database and rapid identification tool for continental Africa. *Taxon* **2014**, *63*, 1159–1164. [CrossRef]
31. Little, E.L. *Common Forest Trees of Hawaii: Native and Introduced*; US Department of Agriculture: North Bend, WA, USA, 1989.
32. Zhang, W.; Qi, J.; Wan, P.; Wang, H.; Xie, D.; Wang, X.; Yan, G. An easy-to-use airborne LiDAR data filtering method based on cloth simulation. *Remote Sens.* **2016**, *8*, 501. [CrossRef]
33. Li, W.; Guo, Q.; Jakubowski, M.K.; Kelly, M. A new method for segmenting individual trees from the lidar point cloud. *Photogramm Eng. Rem. S.* **2012**, *78*, 75–84. [CrossRef]
34. Nurunnabi, A.; Sadahiro, Y.; Lindenbergh, R.; Belton, D. Robust cylinder fitting in laser scanning point cloud data. *Measurement* **2019**, *138*, 632–651. [CrossRef]
35. Vicari, M.B.; Disney, M.; Wilkes, P.; Burt, A.; Calders, K.; Woodgate, W. Leaf and wood classification framework for terrestrial LiDAR point clouds. *Methods Ecol. Evol.* **2019**, *10*, 680–694. [CrossRef]
36. Mahmoudi, M.; Sapiro, G. Three-dimensional point cloud recognition via distributions of geometric distances. *Graph. Models* **2009**, *71*, 22–31. [CrossRef]
37. Raumonen, P.; Casella, E.; Calders, K.; Murphy, S.; Åkerblom, M.; Kaasalainen, M. Massive-scale tree modelling from TLS data. *ISPRS Ann. Photogramm. Remote Sens. Spat. Inf. Sci.* **2015**, *2*, 189–196. [CrossRef]
38. Raumonen, P.; Kaasalainen, M.; Åkerblom, M.; Kaasalainen, S.; Kaartinen, H.; Vastaranta, M.; Holopainen, M.; Disney, M.; Lewis, P. Fast automatic precision tree models from terrestrial laser scanner data. *Remote Sens.* **2013**, *5*, 491–520. [CrossRef]
39. Halloy, S. A morphological classification of plants, with special reference to the New Zealand alpine flora. *J. Veg Sci.* **1990**, *1*, 291–304. [CrossRef]
40. Dansereau, P.; Arros, J. Essais d'application de la dimension structurale en phytosociologie. I. Quel ques exemples Europeens. *Vegetatio* **1959**, *9*, 48–99. [CrossRef]
41. Orshan, G.; Roux, A.L.; Montenegro, G. Distribution of monocharacter growth form types in mediterranean plant communities of Chile, South Africa and Israel. *Bull. De La Société Bot. De France. Actual. Botaniques.* **1984**, *131*, 427–439. [CrossRef]
42. Terryn, L.; Calders, K.; Disney, M.; Origo, N.; Malhi, Y.; Newnham, G.; Raumonen, P.; Åkerblom, M.; Verbeeck, H. Tree species classification using structural features derived from terrestrial laser scanning. *ISPRS J. Photogramm.* **2020**, *168*, 170–181. [CrossRef]
43. Wei, T.; Lin, Y.; Yan, L.; Zhang, L. Tree species classification based on stem-related feature parameters derived from static terrestrial laser scanning data. *Int. J. Remote Sens.* **2016**, *37*, 4420–4440. [CrossRef]
44. Colaço, A.F.; Trevisan, R.G.; Molin, J.P.; Rosell-Polo, J.R. A method to obtain orange crop geometry information using a mobile terrestrial laser scanner and 3D modeling. *Remote Sens.* **2017**, *9*, 763. [CrossRef]
45. Di Gennaro, S.F.; Matese, A. Evaluation of novel precision viticulture tool for canopy biomass estimation and missing plant detection based on 2.5 D and 3D approaches using RGB images acquired by UAV platform. *Plant. Methods* **2020**, *16*, 91. [CrossRef]
46. Brandtberg, T. Classifying individual tree species under leaf-off and leaf-on conditions using airborne lidar. *ISPRS J. Photogramm. Remote Sens.* **2007**, *61*, 325–340. [CrossRef]
47. Benesty, J.; Chen, J.; Huang, Y.; Cohen, I. Pearson correlation coefficient. In *Noise Reduction in Speech Processing*; Springer: Berlin, Germany, 2009; pp. 1–4.
48. Naidoo, L.; Cho, M.A.; Mathieu, R.; Asner, G. Classification of savanna tree species, in the Greater Kruger National Park region, by integrating hyperspectral and LiDAR data in a Random Forest data mining environment. *ISPRS J. Photogramm.* **2012**, *69*, 167–179. [CrossRef]
49. Xi, Z.; Hopkinson, C.; Rood, S.; Peddle, D. See the forest and the trees: Effective machine and deep learning algorithms for wood filtering and tree species classification from terrestrial laser scanning. *ISPRS J. Photogramm. Remote Sens.* **2020**, *168*, 1–16. [CrossRef]
50. Ren, Y.; Zhang, L.; Suganthan, P.N. Ensemble classification and regression-recent developments, applications and future directions. *IEEE Comput. Intell. Mag.* **2016**, *11*, 41–53. [CrossRef]
51. Agatonovic-Kustrin, S.; Beresford, R. Basic concepts of artificial neural network (ANN) modeling and its application in pharmaceutical research. *J. Pharm. Biomed.* **2000**, *22*, 717–727. [CrossRef]
52. Safavian, S.R.; Landgrebe, D. A survey of decision tree classifier methodology. *IEEE Trans. Syst. Man Cybern.* **1991**, *21*, 660–674. [CrossRef]
53. Altman, N.S. An introduction to kernel and nearest-neighbor nonparametric regression. *Am. Stat.* **1992**, *46*, 175–185.
54. Ho, T.K. A data complexity analysis of comparative advantages of decision forest constructors. *Pattern Anal. Appl.* **2002**, *5*, 102–112. [CrossRef]

55. Cortes, C.; Vapnik, V. Support-vector networks. *Mach. Learn.* **1995**, *20*, 273–297. [CrossRef]
56. Chang, C.C.; Lin, C.J. LIBSVM: A library for support vector machines. *ACM Trans. Intell. Syst. Technol. Rev.* **2011**, *2*, 1–27. [CrossRef]
57. Chang, Y.W.; Hsieh, C.J.; Chang, K.W.; Ringgaard, M.; Lin, C.J. Training and testing low-degree polynomial data mappings via linear SVM. *J. Mach. Learn. Res.* **2010**, *11*, 1471–1490.
58. Howley, T.; Madden, M.G. The genetic kernel support vector machine: Description and evaluation. *Artif. Intell. Rev.* **2005**, *24*, 379–395. [CrossRef]
59. Othmani, A.; Piboule, A.; Dalmau, O.; Lomenie, N.; Mokrani, S.; Voon, L.F.C.L.Y. Tree species classification based on 3D bark texture analysis. In *Pacific-Rim Symposium on Image and Video Technology*; Springer: Berlin, Germany, 2013; pp. 279–289.
60. Calders, K.; Disney, M.; Nightingale, J.; Origo, N.; Barker, A.; Raumonen, P.; Lewis, P.; Burt, A.; Brennan, J.; Fox, N. Traceability of essential climate variables through forest stand reconstruction with terrestrial laser scanning. In Proceedings of the SilviLaser 2015, La Grande Motte, France, 28–30 September 2015.
61. Ester, M.; Kriegel, H.P.; Sander, J.; Xu, X. A density-based algorithm for discovering clusters in large spatial databases with noise. In Proceedings of the Second International Conference on Knowledge Discovery and Data Mining, Portland, OR, USA, 2–4 August 1996; Volume 96, pp. 226–231.
62. Zhang, J.; Rivard, B.; Sánchez-Azofeifa, A.; Castro-Esau, K. Intra-and inter-class spectral variability of tropical tree species at La Selva, Costa Rica: Implications for species identification using HYDICE imagery. *Remote Sens. Environ.* **2006**, *105*, 129–141. [CrossRef]
63. Vabalas, A.; Gowen, E.; Poliakoff, E.; Casson, A.J. Machine learning algorithm validation with a limited sample size. *PLoS ONE* **2019**, *14*, e0224365. [CrossRef]
64. Shi, Y.; Skidmore, A.K.; Wang, T.; Holzwarth, S.; Heiden, U.; Pinnel, N.; Zhu, X.; Heurich, M. Tree species classification using plant functional traits from LiDAR and hyperspectral data. *Int. J. Appl. Earth Obs.* **2018**, *73*, 207–219. [CrossRef]
65. MacFarlane, D.W.; Kane, B. Neighbour effects on tree architecture: Functional trade-offs balancing crown competitiveness with wind resistance. *Funct. Ecol.* **2017**, *31*, 1624–1636. [CrossRef]
66. Aiba, M.; Nakashizuka, T. Architectural differences associated with adult stature and wood density in 30 temperate tree species. *Funct. Ecol.* **2009**, *23*, 265–273. [CrossRef]
67. Belgiu, M.; Drăguţ, L. Random Forest in remote sensing: A review of applications and future directions. *ISPRS J. Photogramm.* **2016**, *114*, 24–31. [CrossRef]
68. Kohyama, T.; Suzuki, E.; Partomihardjo, T.; Yamada, T.; Kubo, T. Tree species differentiation in growth, recruitment and allometry in relation to maximum height in a Bornean mixed dipterocarp forest. *J. Ecol.* **2003**, *91*, 797–806. [CrossRef]
69. Poorter, L.; Bongers, L.; Bongers, F. Architecture of 54 moist-forest tree species: Traits, trade-offs, and functional groups. *Ecology* **2006**, *87*, 1289–1301. [CrossRef]
70. Wu, Y.; Zhang, X. Object-based tree species classification using airborne hyperspectral images and LiDAR data. *Forests* **2020**, *11*, 32. [CrossRef]